A novel bioresorbable ultrathin device as a controlled release system for protecting cells from oxidative stress from Alzheimer's disease

Geisa Nogueira Salles[1,2], Fernanda Aparecida dos Santos Pereira[1,2], Cristina Pacheco-Soares[2], Fernanda Roberta Marciano[1], Christian Hölscher[3], Thomas Jay Webster[4,5] and Anderson de Oliveira Lobo[1]*

[1]Laboratory of Biomedical Nanotechnology, Institute of Research & Development (IP&D), University of Vale do Paraiba (UNIVAP), Av. Shishima Hifumi, 2911, 12244-000, Sao Jose dos Campos, SP, Brazil.

[2]Laboratory of Dynamics of Cellular Compartments, IP&D, UNIVAP Av. Shishima Hifumi, 2911, 12244-000, Sao Jose dos Campos, SP, Brazil.

[3]Division of Biomedical and Life Sciences, Faculty of Health and Medicine, Lancaster University, Lancaster LA1 4YQ, UK.

[4]Department of Chemical Engineering, Northeastern University, Boston, MA, USA.

[5]Center of Excellence for Advanced Materials Research, King Abdulaziz University, Jeddah, Saudi Arabia.

***Correspondent author:** aolobo@pq.cnpq.br and lobo.aol@gmail.com.

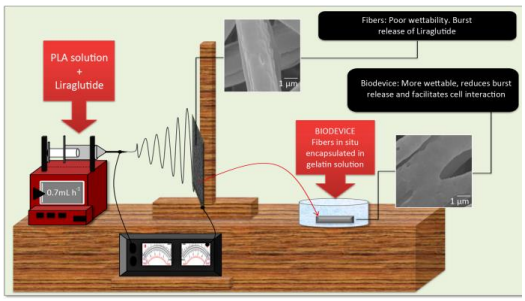

GRAPHICAL ABSTRACT

ABSTRACT

Bioresorbable ultrathin fibers have highly functional features which can~~,~~ preserve drug efficacy, avoiding premature degradation, and control drug release rates over long periods of time. In parallel, it is known that Alzheimer's Disease (AD) has been linked to impaired insulin signalling in the brain. Glucagon-like peptide 1 (GLP-1) analogues have beneficial effects on insulin release and possess great neuroprotective ~~effects~~properties. Herein, we describe for the first time the incorporation of a GLP-1 analogue, Liraglutide, into poly (lactic acid) (PLA) ultrathin fibers with *in situ* gelatin capsules, in order to provide the controlled release of Liraglutide, improving neuroprotective properties. In this study, PLA, a bioresorbable polymer in which degradation products have neurogenesis characteristics, was electrospun and loaded with Liraglutide. Moreover, PLA/Liraglutide fibers were encapsulated with gelatin and were shown to have better properties than the non-encapsulated ~~groups~~ fibers ~~towards the~~in terms of controlled release of Liraglutide, which was accomplished in the present study for up to 60 days. We observed that this biodevice was completely encapsulated with gelatin, which made the material more hydrophilic than PLA fibers alone and the biodevice was able to enhance fibroblast interaction and reduce mitochondrial stress in a neuroblastoma cell line. In this manner, this study introduces a new material which can improve neuroprotective properties from AD oxidative stress via the sustained long-lasting release of Liraglutide to a neuroblastoma cell line.

KEYWORDS: Ultrathin fibers; Drug delivery; Sustained release; Liraglutide; Alzheimer's disease; Biodevice.

1. Introduction

Nano and ultrathin fibers have been considered ~~essential~~ promising candidates for numerous drug delivery systems [1-3]. For the treatment of~~Focused on~~ brain pathology, polymeric fiber~~,~~ based drug controlled systems have promising properties due to their ability to release drugs into circulation over long time periods, providing for time-dependent mechanical properties and modulating the release of bioactive agents [4]. Such properties have led to

consequentially (what do you mean by this?) ~~favorable~~ efective drug bioresorbable delivery across the blood brain barrier (BBB) [5, 6], protecting its interaction (of what?) from within the brain [7]. Besides, the use of poly (lactic acid) (PLA) fibers in the brain has recently demonstrated neurogenesis and vascularization of damaged brain tissue [8]. It is further known that self-assembling nanofibers have potential for being useful in Alzheimer's Disease (AD) therapy [9, 10].

Concerning AD, Type 2 Diabetes Mellitus (T2DM) is considered a risk factor for this dementia type [11, 12]. In the brain, insulin deficiency plays an important role in the process of synaptic loss and cognitive reduction [13], thus~~,~~ affecting cellular metabolism, gene expression and neuronal repair systems [14].

GLP-1 (glucagon-like peptide-1) is an endogenous incretin hormone that potentiates insulin secretion, administered to patients with T2DM [15]. An important advantage of GLP-1 and its analogues, such as Liraglutide, is that they do not affect blood glucose levels of normal glycaemic organisms [16]. Furthermore, GLP-1 receptors are expressed by neurons [17] and have longer biological half-lives in the organism (the receptors?) [18]. They are also capable of crossing the BBB, inducing neurogenesis, providing beneficial effects and delaying ageing of the brain [19].

Consequently, the stimulation of the GLP-1 receptor represents a promising technique to improve impaired brain function in patients with AD [20, 21]. For this, ultrathin fibers containing GLP-1 analogues may potentiate the therapeutic effects of this peptide for AD, especially because the peptide might be maintained ~~in~~ at constant ~~circulation,~~concentrations over a long time period, continually reaching the BBB, improving drug performance in the brain. In the literature there appears to be no *in vitro* and/or *in vivo* studies that researched the association of ultrathin fibers with the aforementioned therapy for AD.

Promisingly, in this study we incorporated ~~a~~ Liraglutide ~~commercial analogue~~ (Victoza®) into bioresorbable ultrathin PLA fibers encapsulated with gelatin, creating a biodevice able to provide sustained and long-lasting release of the drug for AD treatment. The developed materials were further characterized and tested *in vitro*. Again, this therapy is very ~~attractive~~promising~~,~~ ~~once~~ if the biodevice provides ~~Liraglutide~~ sustained release of Liraglutide, combining advantages of the drug with suitable mechanical properties, bioactive surfaces and controllable degradability of the materials. Importantly, our biodevice was non-toxic to fibroblasts and able to release ~100nM (do you mean nmol? nM is a concentration) of

Formatted: Font color: Red

Formatted: Font: Font color: Black, Pattern: Clear (White)

Liraglutide per day, improving neuroblastoma viability for 1, 2 and 7 days reducing mitochondrial oxidative stress that can result from AD.

2. Experimental

2.1 Materials

PLA (Ingeo® 2003D) was purchased from NatureWorks. The solvents used in this study were N,N-dimethylformamide (DMF, Sigma-Aldrich, ≥ 99%) and chloroform (Sigma-Adrich, ≥ 99%). Liraglutide was purchased from Novo Nordisk (Victoza®). Gelatin (Type A, from porcine skin), Dulbecco's minimum essential medium (DMEM) and DMEM/F12 (Nutrient mixture F-12) were also acquired from Sigma-Aldrich. Phosphate buffered saline (PBS, pH 7.4) was freshly prepared. Any mention of other chemicals and their respective origin are indicated along the text.

2.1.1 Preparation of PLA and PLA/Liraglutide solutions

PLA was first dissolved in chloroform; the solution was stirred for up to 20 h, at room temperature. After that, 10 µM of Liraglutide was homogenized in DMF, this solution was incorporated into the PLA solution to a final PLA concentration of 10% (w/v) and the resulting mixture (3:1 Chloroform:DMF) was stirred for 1 h. The whole procedure was performed in a hermetically sealed container at 24 ºC ± 2 ºC; relativity humidity at 40 ± 10%.

Another solution was prepared under the same parameters but without Liraglutide (control).

2.1.2 Electrospinning

The prepared solution (previously described in the 2.1.1 section) was sucked into a glass syringe (BD Yale™), and fixed horizontally in a syringe infusion pump (KDS-100, KdScientific). Subsequently, the positive electrode was connected to the needle (Inbras®, 0.7 mm in diameter) attached to the syringe and the negative, to a metallic apparatus (10 cm x 10 cm x 0.3 cm) covered with aluminium foil as a fiber collector (10 cm needle-to-collector distance); both were also connected to a high voltage power

supply (Bertan 230®, 15kV as positive voltage). Electrospinning was carried out for up to 1 h at 24 ± 2 ºC and relative 'humidity at 40 ± 10 % (flow rate of 0.7 mL h^{-1}). Electrospun fibers were collected on the aluminium foil, dried in the vacuum for 3 h and stocked at 4ºC.

2.1.3 *In situ* encapsulation (biodevice assembly)

In situ encapsulation was performed in order to modify the surface of the PLA/Liraglutide fibers, producing our biodevice. For this, gelatin was dissolved in sterile PBS (10% w/v). The solution was stirred for 2 h in a hermetically sealed container at 35 ºC to complete dissolution. After that, at room temperature, 0,2 µM of commercial Liraglutide was added to the gelatin solution and kept under agitation for 30 min in a closed system with controlled atmosphere. The solution was placed in a Petri dish and the PLA/Liraglutide fibers produced (previously described in the 2.1.2 section) were removed from the aluminium foil and immersed into the gelatin solution (10% w/v). Following that, the biodevice was removed and stocked at 4 ºC.

2.2 Characterization

2.2.1 Scanning electron microscopy (SEM) and field-emission scanning electron microscopy (FE-SEM)

The fibers and biodevice morphologies were characterized by both FE-SEM (Lyra3 XM, Tescan®) and SEM (Zeiss EVO MA-10). All samples were coated with a thin layer of gold, using a sputter-coat system (K 550X, EmiTech) before analysis.

2.2.2 Fiber Diameter

The average fiber diameters were measured from the analysis of the SEM micrographs (n=100 fibers), using ImageJ® software. The data were expressed as media and ± standard deviation.

2.2.3 Attenuated Total Reflectance Fourier Transform infrared (ATR-FTIR)

The structure of electrospun PLA and PLA/Liraglutide fibers and Liraglutide was obtained on an ATR-FTIR spectrophotometer (Spotlight-400, Perkin Elmer FTIR Imaging System), in the range from 4000 to 0 cm^{-1}, in transmittance mode.

2.2.4 Wettability (contact angle measurements)

The wetting of aqueous drops on the PLA fibers and biodevice surfaces were characterized using a goniometer (EasyDrop DAS 100S, KRUSS). The measurements were based on the sessile-drop method using aqueous drops at a volume of 2 µL placed on a substrate. Briefly, images of a single drop of deionized (DI) water deposited on PLA fibers and on the biodevice were periodically acquired (every 5 minutes), by a custom setup with a CCD camera. The first contact angle was measured 15 s after the drop casting to ensure that the droplet reached its equilibrium position. In order to estimate the contact angle values, a plugin for the open-source software ImageJ® was exploited [22]. All measurements were carried out in a controlled humidified atmosphere (50 ± 10%). After the wettability assay, it was possible to reach the time it took to the materials completely absorb the DI water drop.

2.2.5 Zeta Potential

The zeta potential is a key indicator of a molecule stability dispersed in a solution. Zeta potential was analyzed by dynamic light scattering (Delsa™ Nano Beckman Coulter, USA). Zeta potential of the peptide was measured by diluting Liraglutide in a DMF solution.

2.3 Liraglutide release *in vitro*

The *in vitro* release of Liraglutide was evaluated by soaking the PLA/Liraglutide fibers (~30 mg) into 30 mL of sterile PBS (pH 7.4) in a hermetically sealed container, which was kept under constant agitation, in a shaker at 37 °C and 75 rpm. At regular time intervals (1, 2, 3, 6, 12, 24, 48, 72, 120, 168, 240, 360, 480, 600, 720 and 1440 h; 0 to 60 days in total), 3 mL of sample were withdrawn and stored at −20 °C until analysis. Then, to the remaining released solution, 3mL of pre-warmed PBS was added after each interval, to maintain the constant volume [23-25]. Subsequently, the amount of Liraglutide in the collected samples was quantified

by UV-visible spectroscopy (DeNovix DS-11), at an absorbance wavelength of 280 nm. PLA fibers (~30mg) without Liraglutide were maintained under the same conditions and the collected periodic solutions were taken to zero the instrument before each regular time interval of analysis.

The amount of Liraglutide present in the release buffer was determined by converting the detected UV absorbance to its concentration according to the calibration curve of known concentrations of Liraglutide in the same buffer (PBS). All solutions were freshly prepared and the absorbance was immediately measured. The cumulative percentage of the released Liraglutide was calculated. The assay was performed in triplicate; data are represented as mean ± standard deviation.

2.4 Therapy with the produced materials

2.4.1 Cell culture

SH-SY5Y cells (a human neuroblastoma cell line) was kindly provided by the Laboratory of Chemical Biochemistry (Biochemistry Department, Universidade Federal do Rio Grande do Sul, BRA) and maintained in DMEM/F12 (1:1), supplemented with 10% FBS and a 1% antibiotic-antimicotic solution at 37°C in a humidified incubator in an atmosphere of 5% CO_2. These cells were used to determine the neurprotective influence of the biodevice after an H_2O_2 oxidative stress challenge indicative of AD.

L929 cells (murine fibroblast, derived from L line; ATCC®CCL-1TM), acquired from the Bank of Cells of Rio de Janeiro - BCRJ (BCRJ: 0188, lot 001 158) were used in order to evaluate cell adhesion on the biodevice and provide general cytotoxicity data. This cell line was cultured using DMEM supplemented with 10% FBS and a 1% antibiotic-antimitotic solution and was further maintained at 37 °C in an atmosphere of 5% CO_2.

2.4.2 Therapy

In order to sterilize the materials (cut with dimensions of 1cm x 1cm), they were quickly immersed in 70% ethanol, followed by sterile PBS and DMEM/F12 medium before being placed in contact with cells.

For each of the following assays, SH-SY5Y cells were seeded and plated at the density of 6 x 10^4 cells/well and then were incubated in a 5% CO_2 humidified atmosphere, at 37 ºC. Cells attained 50-70% confluence within 24 h. Then, cells were serum starved for 12 h in 0.5% FBS DMEM/F12 medium [26]. Subsequently, cells were incubated with the materials for 24 h; after that, materials and medium were removed and cells were stressed by exposed to 5µM H_2O_2 for 1 h.

2.5 Therapeutic effects of the produced materials

2.5.1 Cell viability

SH-SY5Y cells viability was evaluated by the Trypan blue exclusion assay. Materials were incubated within the plated cells (previously described in the 2.4.2 section) and viability was evaluated on days 1, 2 and 7. After H_2O_2 incubation, cells were washed with PBS, trypsinized, centrifuged and the pellet was resuspended in DMEM/F12 medium. Cells were stained with a Trypan blue dye (0.4% diluted in PBS, Sigma-Aldrich) for 5 min. Then, viable cells were counted with the Countess Automated Cell Counter (Life Technology ™) equipment.

2.5.2 Mitochondrial reactive oxygen species (ROS) detection

For ROS fluorescence intensity detection, therapy (previously described in section 2.4.2) was normally performed for 24 h; however, in order to achieve an optimal fluorescence reading, cells were seeded in optical-bottom microplates (Nunc, Thermo Scientific™). This plate had a polystyrene black structure with a film at the bottom of the plate, facilitating a fluorescence reading.

After H_2O_2 incubation, cells were exposed to 5 µM MitoSOX Red (Invitrogen/Molecular probes) for 10 min and washed with PBS. Fluorescence intensity was measured using a fluorescence reader (BioTek®). MitoSOX Red was excited at 485 ± 40 nm and emission was collected at 590 ± 20 nm.

In parallel, for the immunofluorescence imaging of MitoSOX Red, therapy (previously described in section 2.4.2) was normally performed. Afterwards, cells were labelled with MitoSOX Red, as previously described and the nuclei were stained using DAPI.

Photomicrographs were acquired using a fluorescence microscope (Leica Epifluorescence Microscope DMLB with a camera to capture pictures; model Leica DFC310FX).

2.6 Cell adhesion on the biodevice

The L929 cell line was used to verify cellular adhesion on the materials. For this, L929 cells (6 x 10^4 cells/well) were cultivated on the materials (cut to dimensions of 1cm x 1cm), for 24 h, in a 5% CO_2 humidified atmosphere, at 37ºC. After that, L929 cells were fixed with 4% paraformaldehyde/2.5% glutaraldehyde (Sigma-Aldrich) solution for 10 min. The adherent cells were dehydrated using the following sequences of acetone/DI mixture (10 min each): 10, 30, 50, 70, 90 and 100% (v/v). Then, samples were immersed in 100% acetone/hexamethyldisilazane (HMDS) (Sigma-Aldrich ≥99%) (1:1) and finally in HMDS, both for 10 min. All procedures were performed at room temperature. The materials were dried at room temperature, sputter-coated with a thin layer of gold (~10 nm) and subjected for SEM analysis. To quantify cell spreading area, micrographs were converted to black-and-white images using ImageJ software and the area of each cell was then measured.

2.7 Statistical analysis

Results were expressed as the mean ± standard deviation. Statistical analysis were performed by the unpaired Student's *t* test and one-way ANOVA, followed by a Bonferroni *post hoc*, for multiple comparison, using the Prism 5.0 (GraphPad Inc. USA); $p < 0.05$ was considered to be statistically significant.

3 Results and Discussion

In this study, a novel ultrathin PLA/Liraglutide/gelatin biodevice was synthesized. It was characterized and experimentally tested for AD therapy *in vitro*, enhancing Liraglutide long-sustained release. This achievement has great potential, since AD is a chronic disease and,

currently, all symptomatic treatments are intrinsically long-term and dependant on daily medication.

Liraglutide was loaded into the PLA fibers by using a simple mixture, both peptide and polymer were electrospun together, a very important asset for drug delivery systems and the generation of a three dimensional functional biological structures. This drug delivery method allows simple diffusion of the peptide, which is characterized by an initial burst release by simple diffusion, followed by a long period of sustained release, according to polymeric degradation [4, 27].

Focusing on releasing drugs in a controlled sustained manner, we encapsulated the fibers by introducing a sheath layer of gelatin around them, which also contained Liraglutide, but at a lower concentration, in order to control the initial burst release from the fibers. Therefore, the capsule created a hydrophilic drug-loaded external layer, exposed on the top of the biodevice, which permitted better biological interaction and loaded the correct amount of drug. This accomplishment may provide sustained release from the first contact with the organic fluid, once the gelatin prevents the films from disintegration or shear forces under physiological conditions [28].

Besides, the surface modification of our PLA/Liraglutide fibers using the gelatin capsule was a method to introduce better biofunctionality to the material, making it more biochemically and structurally similar to the tissue [29].

Fig. 1 shows SEM and FE-SEM micrographs of the evaluated materials (PLA and PLA/Liraglutide fibers and the biodevice). Fig. 1A demonstrates that PLA fibers did not present beads or defects. Clearly, there was a distinct rough surface in PLA/Liraglutide fibers (Fig. 1B). From this, it can be morphologically assumed that Liraglutide was successfully incorporated into PLA fibers. Fig 1C exhibits the biodevice morphology, gelatin capsule can be well observed.

Fig. 1 also demonstrates histograms of the diameter distribution (n=100). As expected, PLA fibers diameter (738.044 ± 74.74 nm) slightly increased once Liraglutide was incorporated into them (1055.75 ± 131.69 nm) and increased even more with gelatin capsules (1389.56 ± 267.34 nm), which in turn may be responsible for their more heterogeneous diameter (Fig 1.A1,1.B1 and 1.C1, respectively).

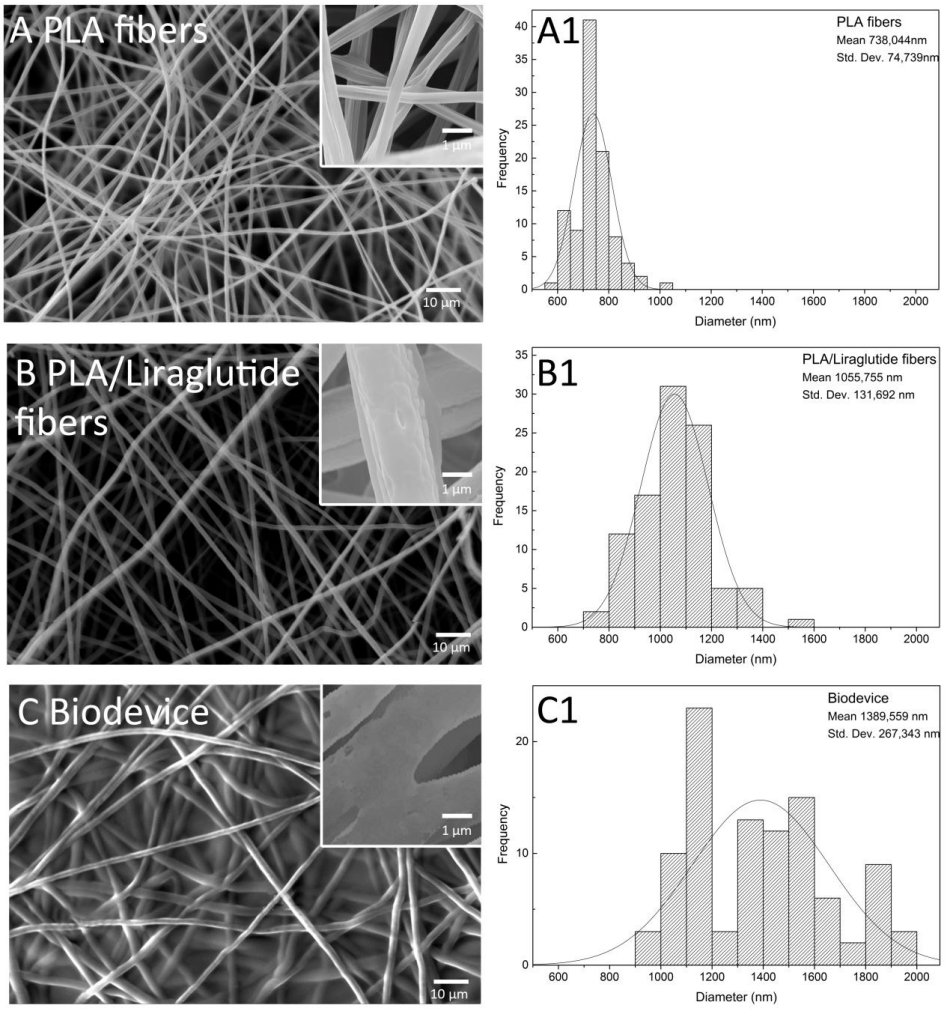

Fig. 1: SEM and FE-SEM micrographs of (**A**) PLA fibers, (**B**) PLA/Liraglutide fibers and the (**C**) Biodevice. Histograms of the PLA diameter distribution collected from SEM micrographs from (**A1**) PLA fibers, (**B1)** PLA/Liraglutide fibers and the (**C1**) Biodevice; (n=100 fibers for all groups).

To further identify the chemical structure of the material, FTIR spectra were recorded in the range from 4000 to 0 cm^{-1} (Fig. 2A). Clearly, it was observed that Liraglutide is present within the polymeric chains of the PLA/Liraglutide fibers (Fig. 2A). We can assume that due to the presence of carboxylic acid C=O symmetric stretching vibrations peaks of Liraglutide, mainly

represented at 1632 cm^{-1}, (characteristically for amino acid chains [30-32]) and an N-H stretching band (3410 cm^{-1}) [33, 34]. Both were observed in Liraglutide and PLA/Liraglutide fibers spectra. The data support that Liraglutide was well-loaded and was kept intact within the fibers, since the same absorption bands are shown for both the Liraglutide and PLA/Liraglutide scaffolds.

The successful sustained drug release from polymeric fibers has been considered an important parameter for investigation [4]. It is known that poly (L-lactic acid)/poly (lactic-co-glycolic acid) (PLLA/PLGA) electrosprayed particles are able to release drugs for 30 days [35]. Liraglutide release behavior from PLA/Liraglutide fibers was investigated at pH 7.4 (Fig. 2B). We observed that our PLA/Liraglutide fibers were able to release Liraglutide for over 60 days.

As shown and expected (Fig. 2B), our release profile has two main characteristics: a burst release stage for the first week, especially for the first 24h followed by a slow, well-controlled and linear release (from 7 to 60 days respectively), maintained at ~100nM per day (~1% of Liraglutide content in the fibers released per day), which is ideal for our *in vitro* model [26]. The burst release of a high amount of loaded Liraglutide from the fibers within the first week was mainly due to the diffusion of Liraglutide dispersing around the fibers. The gelatin capsule was able to improve this 7 days burst release; however, although Liraglutide released from the biodevice could not be quantified by a UV spectrophotometer, due to the gelatin density and its absorption band, we confirmed gelatin efficiency by different surface wettability measurements (Fig. 2C).

Fig. 2C and D indicated the wettability scheme of PLA fibers and the biodevice, respectively, showing snapshots and contact angle measurements every 5 min until the time it took to completely absorb a drop of DI water into the samples. The contact angle of droplets provides a measure of wettability of the substrate on which they sit, indicating whether the wetting of the substrate is increased or not [36]. The initial contact angle of PLA fibers was 156.467º (±1.457º) while for the biodevice, the angle was much lower (49.9º ±0.959º). The DI water drop was fully absorbed by PLA fibers after 60 min, while biodevices took no more than 30 min. These differences in wettability indicated that hydrophilicity increased once fibers were encapsulated with gelatin. Based on this result, it is suggested that the *in situ* gelatin capsule

represents a promising solution for poor wetting of PLA fibers, increasing its biological interaction [37].

Zeta potential plays an important role in overall drug physical stability. Zeta potential indicated that, once in suspension, Liraglutide interacts well with the fluid electrospinning solution (-19.01mV), this measurement corroborates with the one described by Kaasalainen *et al.* (2012) [38], indicating that the peptide may be biologically stable and functional.

Encapsulation efficiency and burst release are two related parameters showing how effectively the drug is captured and released within the polymer [39]. The capsule was able to enhance drug-encapsulation efficiency, better controlling the release of the drug and reducing the burst release in the first week.

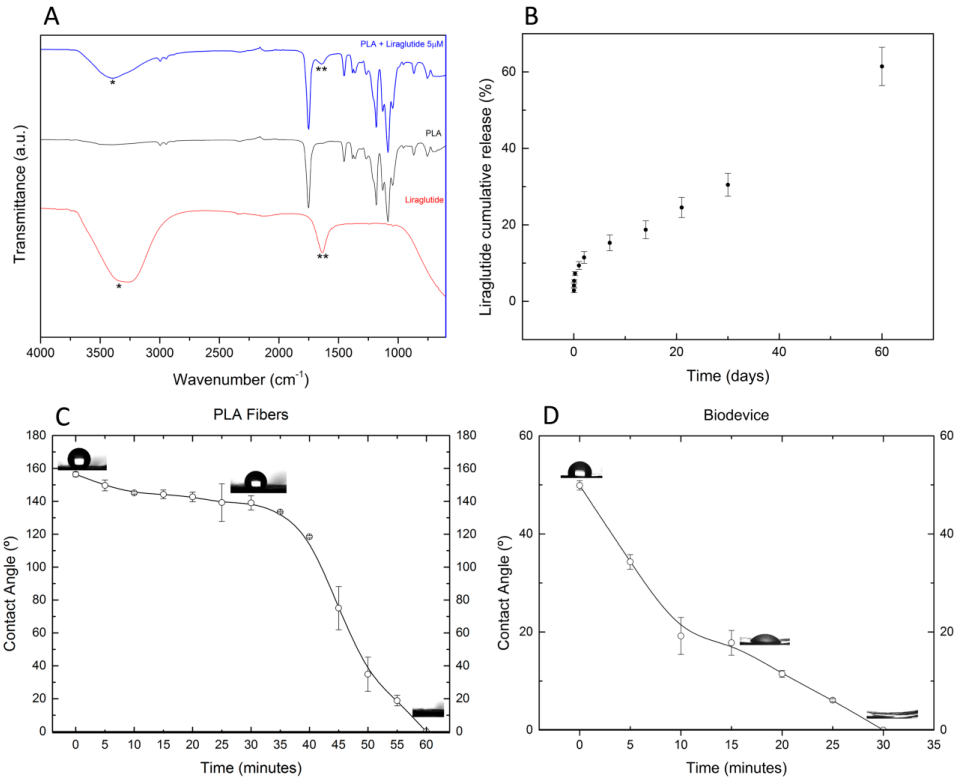

Fig. 2: Characterization of the produced materials. **(A)** ATR-FTIR spectra of: PLA/Liraglutide fibers; PLA fibers and Liraglutide, respectively. * and ** refers to the peptide bands, 1632 and 3410 cm^{-1} wavenumber, respectively. **(B)** Cumulative percentage *in vitro* release of Liraglutide

from PLA/Liraglutide fibers immersed in PBS at pH 7.4. **(C and D)** Contact angle and wettability scheme of the PLA fibers and biodevice, respectively.

Fig. 3 shows cell viability measured using the Trypan blue exclusion assay up to 7 days. All materials maintained higher cell viability than the stressed group in all periods of incubation. H_2O_2 induced stress represents the stress that neurons are exposed to in AD.

Sharma *et al* (2014) [26] described that Liraglutide has neuroprotective effects on SH-SY5Y viability when oxidatively stressed, reducing an inflammatory response [40]. Our results corroborate with theirs in that the amount of cells only stressed with H_2O_2 was much lower. However, once cells were pre-treated with the materials and then stressed, it was observed that PLA fibers containing Liraglutide and the biodevice were not cytotoxic and significantly increased SH-SY5Y viability ($p<0.001$), 24 and 48h after treatment. Curiously, PLA not containing Liraglutide also maintained SH-SY5Y viability, *especially* (Do you mean 'perhaps'?) because the L-lactate released by PLA fibers degradation is required to maintain the metabolism and self-renewal of neurogenic progenitors [41]; generates angiogenesis [42] facilitating neurogenesis and vascularization of a damaged brain [8]. After 7 days, the percentage of stressed cells was much lower, but cells treated with the biodevice showed a considerable higher viability, indicating that the release of Liraglutide was highly controlled and the biodevice was efficiently treating the cells, improving their viability.

Formatted: Font: (Default) Arial, 10 pt

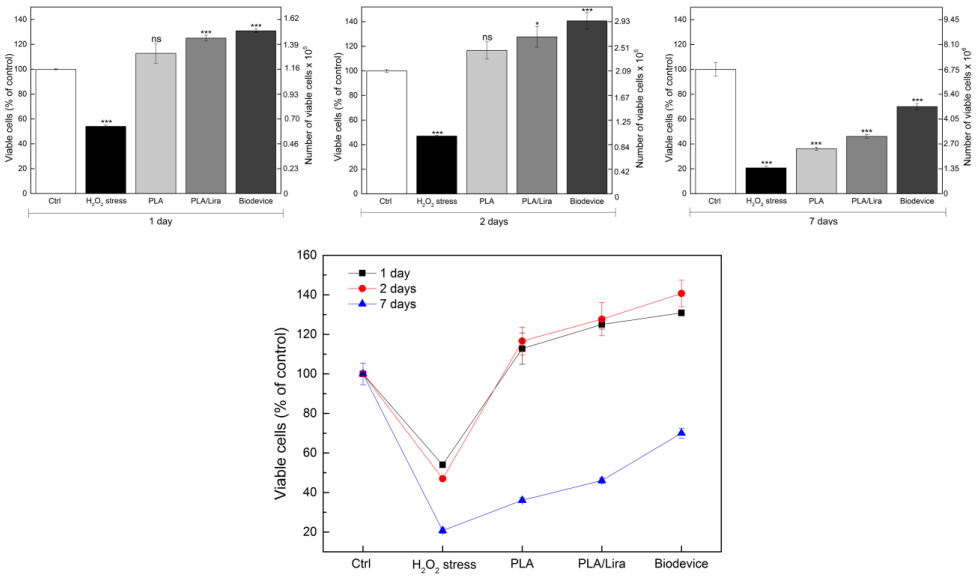

Fig. 3: Viability of SH-SY5Y cells pre-treated with the developed materials and stressed with H_2O_2. **(A)** Cells were pre-treated with PLA fibers; PLA/Liraglutide fibers, biodevice and materials were allowed to be in contact with the cells for 1 day and H_2O_2 stress was performed after that. **(B and C)** Same groups were evaluated, but the materials were kept in contact with the cells for 2 and 7 days, respectively, and H_2O_2 stress was performed every 24h. **(D)** Comparison between different incubation periods ($^{*}p<0.05$ and $^{***}p<0.001$; ns non-significant *vs* control).

We examined mitochondrial ROS levels of SH-SY5Y cells with MitoSOX Red fluorescent, which is a live-cell permeant probe that selectively targets mitochondria and exhibits bright red fluorescence when oxidized by superoxides [43]. It was observed that the pre-treatment with Liraglutide and biodevice significantly reduced superoxide generation in the mitochondria of SH-SY5Y stressed with 5µM H_2O_2 (Fig. 4). (Non-significant for Liraglutide and $p<0.001$ for the biodevice). All treated groups showed ROS reduction. In imaging, MitoSOx migrated to the nucleus once it was oxidised. Mitochondria are the major source of intracellular ROS [44, 45]. It is well established that mitochondrial dysfunction and oxidative stress play an important role in AD, considered to be an early event in this dementia [46, 47]. The oxidative stress leads to increased ROS production and precedes the onset of AD development [48], supporting a causative importance of mitochondrial dysfunction in AD.

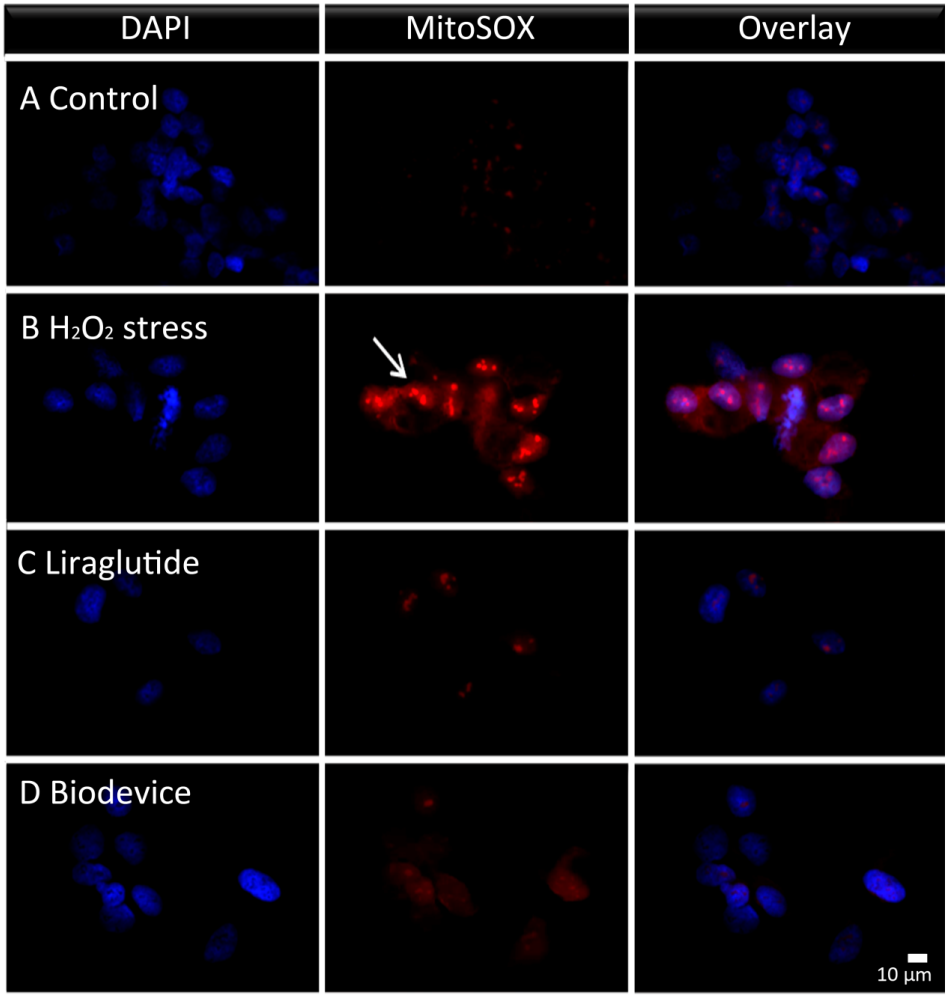

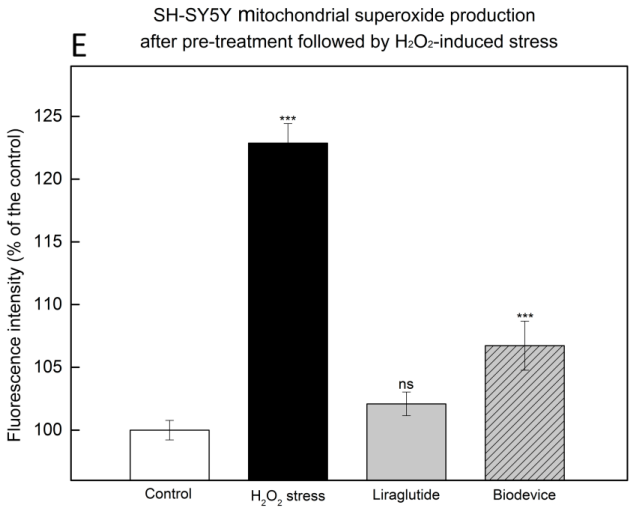

Formatted: Font: (Default) Arial, 10 pt, Bold, Expanded by 0.1 pt, Pattern: Clear (White)

Fig. 4: Reduced mitochondrial ROS levels in SH-SY5Y cells pre-treated with Liraglutide or the biodevice followed by H_2O_2 stress**. (A-D)** Fluorescence microscopy: **(A)** Control; **(B)** 5µM H_2O_2; **(C)** 100nM Liraglutide; and the **(D)** Biodevice. **(E)** Fluorescence intensity of the same groups. White arrow shows the higher intensity of ROS in the stressed group, compared to the other ones ($^{***}p<0.001$ and ns non-significant *vs* control).

L929 cell adhesion to the materials was evaluated in order to verify *in vitro* material implant potential. We also investigated if the gelatin capsule facilitated cellular adhesion (Fig. 5). Fig. 5A shows that the L929 cells efficiently adhered to PLA fibers after 24 h of incubation (cell spreading area 10362 ± 2735 μm^2). However, due to their high hydrophobicity, cells were neither well attached nor diffused as much as observed in Fig. 5B and 5C. In Fig. 5B, it is notable that cells interacted with PLA/Liraglutide fibers (cell spreading area 18976 ± 3613 μm^2). In Fig. 5C, a great interaction between the biodevice and cells was observed (cell area 26408 ± 5081 μm^2), ensuring that this material will be well-fixed once implanted and not induce toxicity to fibroblasts; Fig. 5C also demonstrated that gelatin coating was rough. Fig. 5D represents L929 cell spreading area on the materials, which ensures that wettability certainly influences cell stability and spreading.

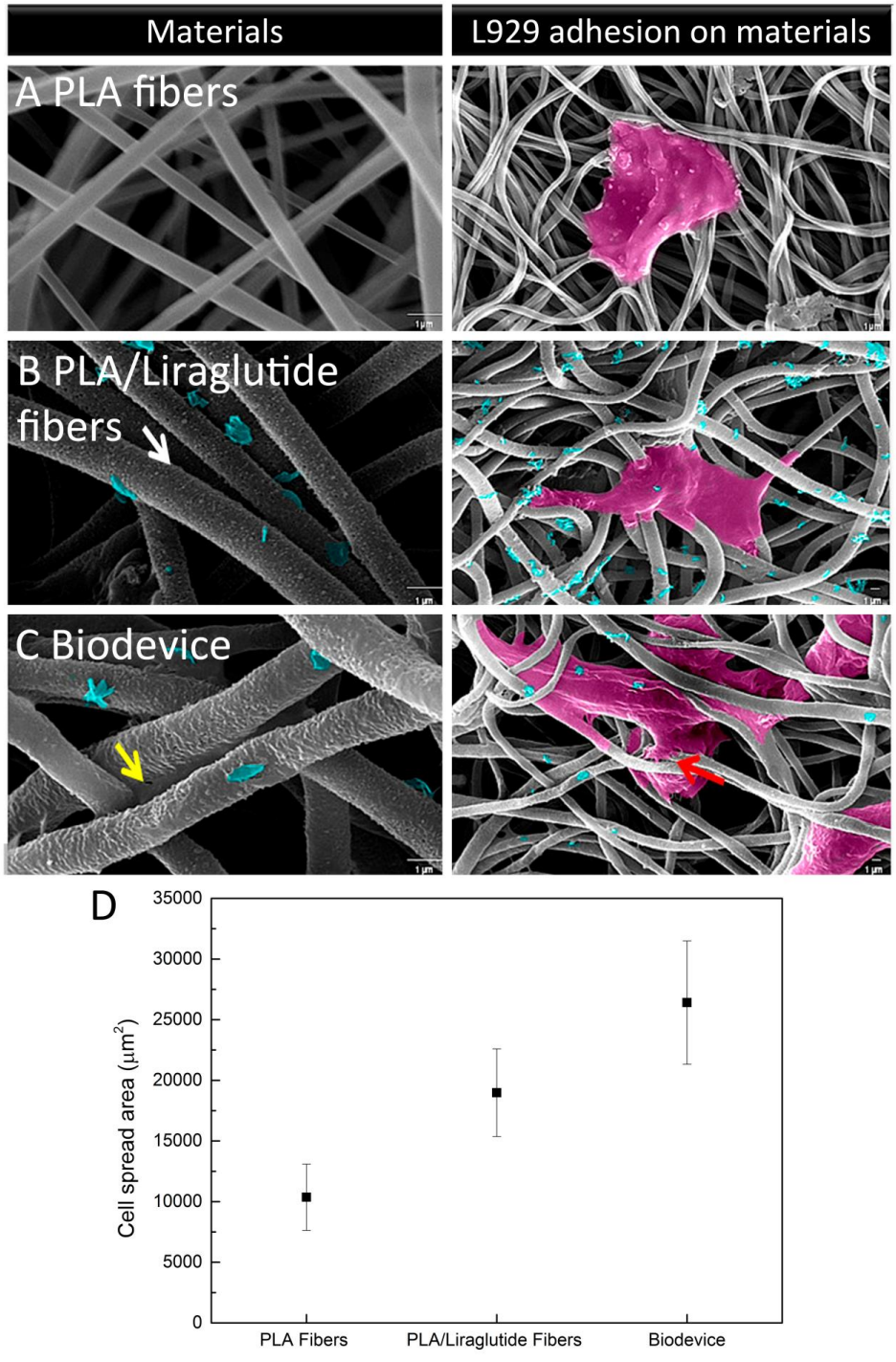

Fig. 5: Material degradation and L929 cell attachment and spreading area after 24h of incubation. **(A)** PLA fibers; **(B)** PLA/Liraglutide fibers; and the **(C)** Biodevice. Images in the left

indicate material degradation, while images in the right show L929 cells adherent to the materials. Cell spreading area on materials. The white **arrow** shows the fiber surface after Liraglutide incorporation; the yellow arrow indicate degraded gelatin and the red arrow~~s~~ shows the ~~great~~ strong interaction between the cell and the biodevice. (Where is the colour in the images coming from?)

Formatted: Underline

Formatted: Underline

It is well stablished that hydrophobicity of electrospun fibers is not good for cell attachment and proliferation, so fiber surface modification which adds hydrophilicity to the material is favorable for cellular interactions [2, 49]. Furthermore, introducing a hydrophilic shell to a hydrophobic polymer produces a highly water-swellable fiber, facilitating drug delivery systems [4]. Fibroblasts are able to produce fibers and amorphous substances, contributing to the healing process and implant reception. They are activated by chemical mediators, which are also responsible for avoiding inflammatory processes and~~,~~ facilitating implant stabilization [50]. The implant, in a short period, is involved (do you mean overgrown?) by fibroblasts and ~~sanguineous~~ blood capillaries in order to maintain stabilized conditions; another group of fibroblasts will then seal the lesion [51].

It is believed that the electrospinning technique employed here brings nano and ultrathin materials closer to clinical applications [52]; and with our results, it is expected that the developed biodevice may provide a new concept of great therapeutic potential for AD. Clearly, gelatin capsules conferred ~~a great approach~~important properties to our drug delivery system, increasing hydrophilicity, facilitating cell adhesion and spreading. Moreover,~~–~~ the capsule maintained Liraglutide integrity and controlled the burst release of the drug to provide a neuroprotective effect.

4 Conclusion

In this study, we propose the ~~concept~~ design of a bioresorbable ultrathin biodevice for the sustained release of Liraglutide as a potential therapy ~~focusing on~~for AD. The developed materials were characterized and tested *in vitro*. We demonstrated that the biodevice has great

conformation (what do you mean by conformation?) and provides a sustained release of the drug for up to 60 days.

Promisingly, our results open up exciting perspectives in the design of implantable devices for AD drug delivery, which could also provide ~~great~~ novel approaches for other chronic disease therapies ~~too~~. Our biodevice allows Liraglutide to easily ~~homogenization~~ homogenize within a PLA solution. Liraglutide incorporation into the fibers was confirmed by FTIR and peptide integrity was observed by zeta potential. The potential of our biodevice was confirmed by wettability measurements, and once fibers were encapsulated with gelatin such wettability increased, which permitted better biological and *in vitro* interactions, increasing neuroblastoma neuroprotective viability, reducing ROS production indicative of AD progression. The strategical (why is it strategical?) biodevice provides a guideline to the development of an implantable material that may represent an important impact for AD therapy.

Acknowledgments

The authors would like to thank the São Paulo Research Foundation (FAPESP, grants 2011/17877-7, 2011/20345-7), the National Council for Scientific and Technological Development (CNPq, 474090/2013-2), the Brazilian Innovation Agency (FINEP – grant 0113042800), the Coordination for the Improvement of Higher Education Personnel (CAPES, grant 88887.095044/2015-00). G. N. Salles would also like to thank FAPESP for the PhD scholarship (2014/20561-0). The authors would like to acknowledge Prof. Fabio Klamt who provided SH-SY5Y cells.

References

1. S. Shalaby, N. Al-Balakocy and S. Abo El-Ola, *Journal of applied polymer science*, 2007, **104**, 3788-3796.
2. L. Jia, M. P. Prabhakaran, X. Qin, D. Kai and S. Ramakrishna, *Journal of Materials Science*, 2013, **48**, 5113-5124.
3. R. Sridhar, R. Lakshminarayanan, K. Madhaiyan, V. A. Barathi, K. H. C. Lim and S. Ramakrishna, *Chemical Society Reviews*, 2015, **44**, 790-814.
4. Y. J. Son, W. J. Kim and H. S. Yoo, *Archives of pharmacal research*, 2014, **37**, 69-78.
5. K. K. Jain, *Nanomedicine*, 2012, **7**, 1225-1233.
6. M. J. Gomes, J. Neves and B. Sarmento, *Int J Nanomedicine*, 2014, **9**, 1757-1769.

7. F. Alexis, E. Pridgen, L. K. Molnar and O. C. Farokhzad, *Molecular pharmaceutics*, 2008, **5**, 505-515.
8. Z. Álvarez, O. Castaño, A. A. Castells, M. A. Mateos-Timoneda, J. A. Planell, E. Engel and S. Alcántara, *Biomaterials*, 2014, **35**, 4769-4781.
9. H. Yang, T. Qu, H. Yang, L. Wei, Z. Xie, P. Wang and J. Bi, *Neuroscience letters*, 2013, **556**, 63-68.
10. H. Yang, H. Yang, Z. Xie, P. Wang and J. Bi, *Neurological research*, 2015, **37**, 84-91.
11. J. A. Luchsinger, M.-X. Tang, S. Shea and R. Mayeux, *Neurology*, 2004, **63**, 1187-1192.
12. M. Ristow, *Journal of molecular medicine*, 2004, **82**, 510-529.
13. M. Suzanne and J. R. Wands, *Journal of diabetes science and technology*, 2008, **2**, 1101-1113.
14. C. Hölscher, *Biochemical Society Transactions*, 2011, **39**, 891-897.
15. J. A. Lovshin and D. J. Drucker, *Nature Reviews Endocrinology*, 2009, **5**, 262-269.
16. T. Perry, H. W. Holloway, A. Weerasuriya, P. R. Mouton, K. Duffy, J. A. Mattison and N. H. Greig, *Experimental neurology*, 2007, **203**, 293-301.
17. A. Hamilton and C. Hölscher, *Neuroreport*, 2009, **20**, 1161-1166.
18. J. J. Holst, *Expert opinion on emerging drugs*, 2004, **9**, 155-166.
19. K. Hunter and C. Hölscher, *BMC neuroscience*, 2012, **13**, 33.
20. C. Holscher, *Recent patents on CNS drug discovery*, 2010, **5**, 109-117.
21. C. Hölscher, *Journal of Endocrinology*, 2014, **221**, T31-T41.
22. A. F. Stalder, T. Melchior, M. Müller, D. Sage, T. Blu and M. Unser, *Colloids and Surfaces A: Physicochemical and Engineering Aspects*, 2010, **364**, 72-81.
23. N. Aboutalebi Anaraki, L. Roshanfekr Rad, M. Irani and I. Haririan, *Journal of Applied Polymer Science*, 2015, **132**.
24. D. Wu, X. Chen, T. Chen, C. Ding, W. Wu and J. Li, *Scientific reports*, 2015, **5**.
25. K. Karthikeyan, R. S. Sowjanya, A. D. Yugandhar, S. Gopinath and P. S. Korrapati, *RSC Advances*, 2015, **5**, 52420-52426.
26. M. K. Sharma, J. Jalewa and C. Hölscher, *Journal of neurochemistry*, 2014, **128**, 459-471.
27. Y. Lu, J. Huang, G. Yu, R. Cardenas, S. Wei, E. K. Wujcik and Z. Guo, *Wiley Interdisciplinary Reviews: Nanomedicine and Nanobiotechnology*, 2016.
28. L. Binan, C. Tendey, G. De Crescenzo, R. El Ayoubi, A. Ajji and M. Jolicoeur, *Biomaterials*, 2014, **35**, 664-674.
29. M. Zamani, M. P. Prabhakaran and S. Ramakrishna, *Int J Nanomedicine*, 2013, **8**, 2997-3017.
30. K. Payne and A. Veis, *Biopolymers*, 1988, **27**, 1749-1760.
31. B. de Campos Vidal and M. L. S. Mello, *Micron*, 2011, **42**, 283-289.
32. T. L. Sellaro, D. Hildebrand, Q. Lu, N. Vyavahare, M. Scott and M. S. Sacks, *Journal of biomedical materials research Part A*, 2007, **80**, 194-205.
33. R. Nyquist, *Spectrochimica Acta*, 1963, **19**, 713-729.
34. C. Amuthambigai, C. Mahadevan and X. S. Shajan, *Optik-International Journal for Light and Electron Optics*, 2016, **127**, 5935-5941.
35. H. Nie, Y. Fu and C.-H. Wang, *Biomaterials*, 2010, **31**, 8732-8740.
36. R. N. Wenzel, *Industrial & Engineering Chemistry*, 1936, **28**, 988-994.
37. E. Bormashenko and Y. Bormashenko, *Langmuir*, 2011, **27**, 3266-3270.
38. M. Kaasalainen, E. Mäkilä, J. Riikonen, M. Kovalainen, K. Järvinen, K.-H. Herzig, V.-P. Lehto and J. Salonen, *International journal of pharmaceutics*, 2012, **431**, 230-236.
39. N. Mangır, A. J. Bullock, S. Roman, N. Osman, C. Chapple and S. MacNeil, *Acta biomaterialia*, 2016, **29**, 188-197.
40. V. Parthsarathy and C. Hölscher, *European journal of pharmacology*, 2013, **700**, 42-50.

41. P. Spéder, J. Liu and A. H. Brand, *Current opinion in cell biology*, 2011, **23**, 724-729.
42. Z. Álvarez, M. A. Mateos-Timoneda, P. Hyroššová, O. Castaño, J. A. Planell, J. C. Perales, E. Engel and S. Alcántara, *Biomaterials*, 2013, **34**, 2221-2233.
43. P. Mukhopadhyay, M. Rajesh, K. Yoshihiro, G. Haskó and P. Pacher, *Biochemical and biophysical research communications*, 2007, **358**, 203-208.
44. A. A. Starkov, *Annals of the New York Academy of Sciences*, 2008, **1147**, 37-52.
45. A. J. Kowaltowski, N. C. de Souza-Pinto, R. F. Castilho and A. E. Vercesi, *Free Radical Biology and Medicine*, 2009, **47**, 333-343.
46. P. Moreira, S. Cardoso, M. Santos and C. Oliveira, *Journal of Alzheimer's Disease*, 2006, **9**, 101-110.
47. B. Su, X. Wang, A. Nunomura, P. I. Moreira, H.-g. Lee, G. Perry, M. A. Smith and X. Zhu, *Current Alzheimer Research*, 2008, **5**, 525.
48. A. Nunomura, G. Perry, G. Aliev, K. Hirai, A. Takeda, E. K. Balraj, P. K. Jones, H. Ghanbari, T. Wataya and S. Shimohama, *Journal of Neuropathology & Experimental Neurology*, 2001, **60**, 759-767.
49. W. J. Li, K. G. Danielson, P. G. Alexander and R. S. Tuan, *Journal of Biomedical Materials Research Part A*, 2003, **67**, 1105-1114.
50. F.-Y. Teng, C.-L. Ko, H.-N. Kuo, J.-J. Hu, J.-H. Lin, C.-W. Lou, C.-C. Hung, Y.-L. Wang, C.-Y. Cheng and W.-C. Chen, *Bioinorganic Chemistry and Applications*, 2012, **2012**, 9.
51. J. Carneiro and L. Junqueira, *Histologia básica: texto, atlas*, Guanabar-Koogan, 2008.
52. W.-E. Teo, R. Inai and S. Ramakrishna, *Science and Technology of Advanced Materials*, 2016.